



## **Development of a Compact and Multifunctional Sensor Array**

S. Reshetnikov, S.D. Wolter and J.T. Glass, Department of Electrical and Computer Engineering, Duke University, Durham. NC 27708 USA

### **Abstract**

This study focuses on using the capability of electrochemical sensor arrays to discretely activate and monitor the response of arrayed electrodes to a redox couple. The Au electrodes were arranged in a 2x5 configuration and activated separately at different potentials. The current levels associated with redox events for ferrocyanide in aqueous solution were measured. The redox couple was also used to assess the electrode impedance by varying polarization potentials and applied frequencies. Both the potentiometric and impedometric methods of operation led to determining the formal potential of ferrocyanide in approximately ten seconds. The ability to ascertain this important electrochemical characteristic in mere seconds is an essential first step in developing an algorithm for a fast and responsive sensor system.

## 1. Introduction

Sensor systems have wide-ranging environmental and bio-security applications. They require many levels of development, from engineering sensor electrode(s) for sensitive and selective response, to the systems level, where signals must be transduced, processed, and networked. Such systems have been used in detection of everything from nitric oxide to the quality of fruit.<sup>1</sup> For instance, Krommenhoek et al. focused on amperometrically monitoring oxygen concentration, conductivity, and pH using an ultra-microelectrode array<sup>2</sup>. Similarly, Chang et. al developed a novel method for an amperometric array sensor platform by employing arrays of sensors in a 24-well cell culture plate for simultaneous in vitro determination of nitric oxide (NO) and superoxide free radicals ( $O^{2-}$ ) produced by stimulated cells.<sup>3</sup> In the present study, we hope to likewise develop an amperometric sensor—exploiting the concurrent accessibility to multiple electrodes.

The Multichannel Microelectrode impedance Analyzer (MMA, Scribner & Associates Inc.) will allow for the robust capability of being able to apply different polarization potentials to numerous electrodes and simultaneously measure the current as well as impedance responses on those electrodes. In fact, the MMA has been previously employed successfully in corrosion studies<sup>4</sup> and as a multichannel potentiostat.<sup>5</sup> Here, it will likewise be used as a multichannel potentiostat to apply DC and AC voltages to multiple electrodes at once. This will allow the rapid acquisition of valuable electrochemical information.

The standard reversible reduction/oxidation (redox) couple, ferro-/ferricyanide ( $Fe(CN)_6^{4-/3-}$ ), has been used in these trials. The main electrochemical parameter that was determined is the formal potential of the  $Fe(CN)_6^{4-}$  reaction:  $Fe(CN)_6^{4-} \leftrightarrow Fe(CN)_6^{3-} + e^-$ . It is the  $E^{0'}$  term in the Nernst Equation:

$$E = E^{0'} - \frac{RT}{nF} \ln \frac{C_O}{C_R} \quad (1)$$

where  $E$  is the polarization voltage,  $F$  is Faraday's constant (96,485 C / mol),  $R$  is the universal gas constant (8.314 J / mol K),  $T$  is the temperature (K),  $C_O$  is the concentration of oxidized species in solution, and  $C_R$  is the concentration of reduced species in solution. The formal potential is also defined as the potential where there is an equal number of oxidized and reduced species of a redox couple on the surface of an electrode.<sup>6</sup> As seen in Equation 1, when  $C_O$  is equal to  $C_R$ , the natural logarithm becomes 0 resulting  $E = E^{0'}$ . Redox couples are differentiated by their formal potentials. Thus, finding the  $E^{0'}$  serves as an initial step in a sensor system that could rapidly ascertain a certain element within an aqueous environment. In the present study, the formal potential was determined using the MMA and confirmed using literature values.

Previous studies employed varying cyclic voltage (CV) scan rates to find the rate that estimates the formal potential most accurately.<sup>7</sup> Instead of using just one electrode, the two methods tested here employ multiple electrodes for rapid formal potential determination. The first method utilizes the half wave potential ( $E_{1/2}$ ), which is the voltage that corresponds to the midpoint of the static potentials at which the maximum and minimum currents occur. Since the diffusion coefficient is approximately the same for both ferro- and ferri-cyanide, then  $E_{1/2}$  is nearly identical to the formal potential of the couple.<sup>6</sup> Furthermore, different polarization potentials can be applied to the ferrocyanide solution to determine which potential results in the lowest measured impedance.<sup>8</sup> It is expected that a polarization voltage equal to the formal potential should correspond to the minimum impedance.

Ultimately, different voltages will be applied simultaneously to multiple electrodes in order to quickly ascertain the formal potential. The  $E^{0'}$  will be found in mere seconds rather than the several minutes it takes to conventionally determine it using CV scans. Significantly

diminishing the time it takes to find the formal potential is the main objective in the development of this rapid sensor array.

## **2. Experimental**

### *2.1 Sensor array preparation*

The sensor array was fabricated using a low temperature co-fired ceramic (LTCC), which allows for flexibility in the design of device structures. The ten Au working electrodes were embedded in the LTCC layers, arranged in a 2x5 pattern, and packaged in a portable via card. Each electrode had an area of approximately 0.5 mm<sup>2</sup> with a distance of 0.5 mm between neighboring electrodes.<sup>9</sup> The Au working electrodes were connected to Au metal lines that were encapsulated within the LTCC. These metal strips were exposed at the edge of the LTCC sensor device and served as the connector junction to the Multichannel Microelectrode Analyzer (MMA).

The working electrode card was placed into a three-electrode electrochemical cell containing a maximum capacity of 30 mL. In the experiments, 25 mL of the cell were filled with a test solution containing 4 mM potassium ferrocyanide hydrate crystal ( $K_4Fe(CN)_6 \cdot 3H_2O$ , Mallinckrodt AR). The charge carrier in the solution was 0.1 M potassium chloride (KCl) crystal (J.T. Baker). A Ag/AgCl reference electrode (Microelectrodes, Inc.) along with a platinum wire counter electrode<sup>10</sup> were also configured into the electrochemical cell. Ultimately, the MMA was connected to the working electrodes via a card edge connector and to the counter and reference electrodes using the standard wire connectors.

Figure 1 shows the overall experimental system setup. The MMA potentiostat employs a high-input impedance circuit to measure the potential between the working and reference electrodes. The current is measured flowing through the whole system and is connected by the

solution between the working and counter electrodes.<sup>6</sup> The MMA has the ability to acquire current response from multiple electrodes with the application of multiple potentials. Moreover, it can acquire the impedance of the testing solution and electrodes at different frequencies. Different polarization potentials can also be applied to different electrodes concurrently to acquire impedance values.

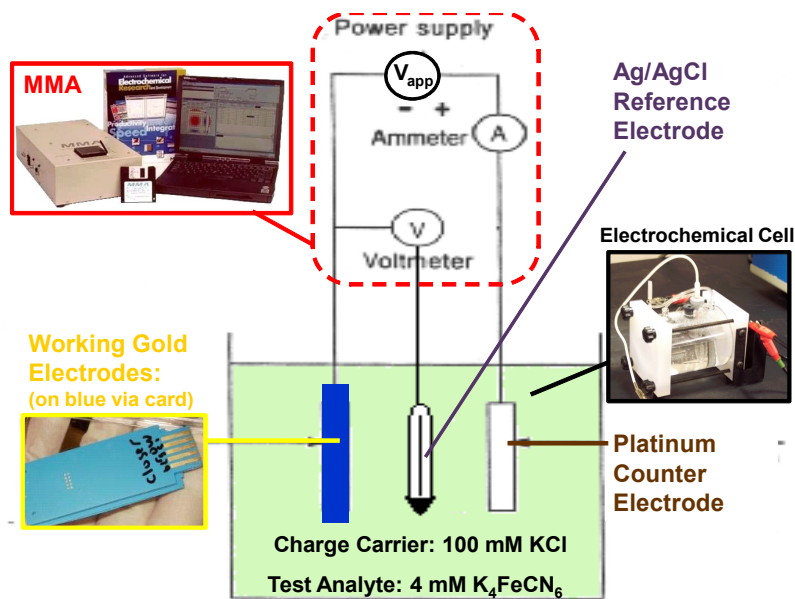


**Figure 1.** Experimental System Setup

## 2.2 Electrochemical measurement procedure

Cyclic voltammetry (CV) sweeps were performed for all electrodes simultaneously in order to determine the approximate formal potential,  $E^0$ , and for comparison of electrode operating characteristics. Sweep rates of 10-100 mV/sec were obtained to quantify the time required to determine  $E^0$  using conventional voltammetry. Next, the crosstalk between proximal electrodes was tested to provide information on concurrent measurement accuracy. This was done by applying 240 mV (approximate formal potential according to CV scan) to all ten electrodes.<sup>10</sup> For simultaneously operating electrodes in sensor platforms as described herein,

the hemispherical volume over each electrode is differentiated from the bulk solution due to reduction and/or oxidation processes. If the electrodes are spaced too closely based on diffusion kinetics this could affect electrode measurements and cause error in sensor function. In this experiment each electrode was polarized to 240 mV separately, one at a time. The current response of individual electrode operation was compared to electrode function in the fully energized array. Lastly, variations in the magnitude of applied potentials,  $\Delta E$ , were examined with regard to accurately determining the formal potential. The MMA acquired current data during these 60 seconds and stored to a data file for later processing.

Impedometric data was collected with DC bias offsets targeting the formal potential of the redox reaction for ferrocyanide. Linear impedance sweeps were done at frequencies from 1 kHz to 1 Hz at DC bias offsets ranging from 0 to 300 mV with an amplitude of 10 mV.<sup>11</sup> In order to establish a voltage offset, a potential was held at the desired value for 10 seconds before beginning the AC voltage application. In order to find the formal potential more quickly, a sweep of 17 to 15 Hz was done with offsets from 130 mV to 310 mV obtaining measurements from multiple electrodes concurrently. In this case, each offset voltage was held for 5 seconds before starting the impedance sweep.

### **3. Results**

#### *Cyclic voltammetry:*

First, cyclic voltammograms (30 mV/s sweep rate) were acquired with the MMA for all the electrodes with two of the sweeps shown in Figure 2. The reversible couple behavior was evident, since the forward and reverse peak currents were nearly identical at 0.01 A/cm<sup>2</sup>.<sup>6</sup> As shown in the figure, the formal potential was assessed at  $\sim +0.24$  V by finding the midpoint between the maximum and minimum currents.<sup>12</sup> Furthermore, the  $\Delta E$  (voltage difference

between peak currents) was found to be approximately 105 mV which matches  $\Delta E$ 's found in similar experiments.<sup>11</sup>

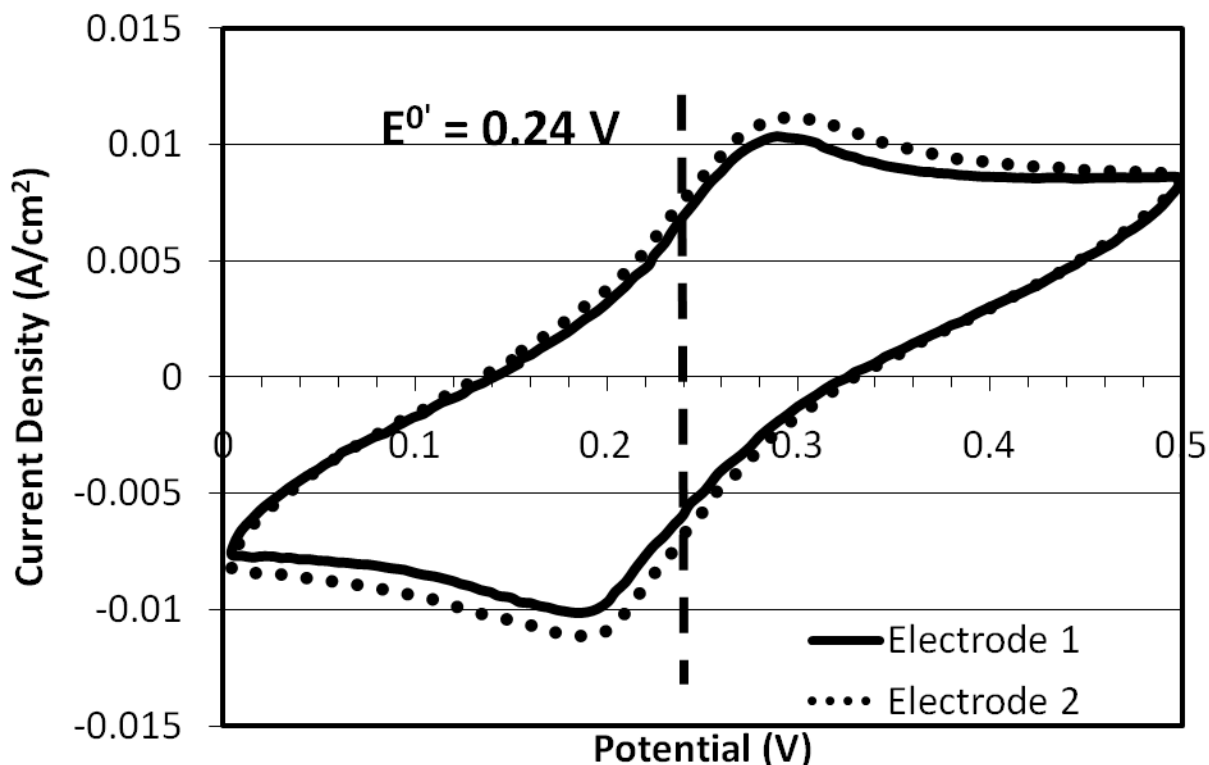


**Figure 2.** Cyclic Voltammetry Sweeps for Two Electrodes Done Simultaneously

*Crosstalk check:*

In addition to the double layer capacitance that forms at the interface of each electrode and solution, a type of diffusion layer materializes with a constant voltage application.<sup>13</sup> The layer arises as a result of  $\text{Fe}(\text{CN})_6^{4-}$  oxidizing to form  $\text{Fe}(\text{CN})_6^{3-}$ , which causes a single electron to migrate into the gold electrode—this allows the MMA to measure a faradaic current.<sup>6</sup> In order to test whether crosstalk exists between proximal electrodes, constant voltages of 240 mV (approx equal to  $E^{0'}$ ) were applied to all electrodes at once and to each electrode individually; the

variation between the I-V curves of the same electrode that did and did not have neighboring ones activated in two trials is displayed in Figure 3. The two plots appear to be comparable and show the same curvature or time constant element. With the application of best-fit models, it was found that the exponential fit applied from 1 to 5 seconds was  $i(t) = 0.0086e^{-0.2483t}$  (single electrode turned on) and  $i(t) = 0.0081e^{-0.2481t}$  (all electrodes turned on). This corresponded to a percent error of 6.2% for the magnitude constant of exponential fits between the two and only 0.07% for the power constant. Furthermore, the second best-fit model from 0.5 to 10 seconds resulted in  $i(t) = 0.0074t^{-0.6356}$  (single electrode turned on) and  $i(t) = 0.0071t^{-0.6371}$  (all electrodes turned on). The magnitude constant in this case had a percent error of 4.6%, while the power constant had a percent error of only 0.24%. All in all, with such small percent errors, there appears to be negligible crosstalk between proximal electrodes.

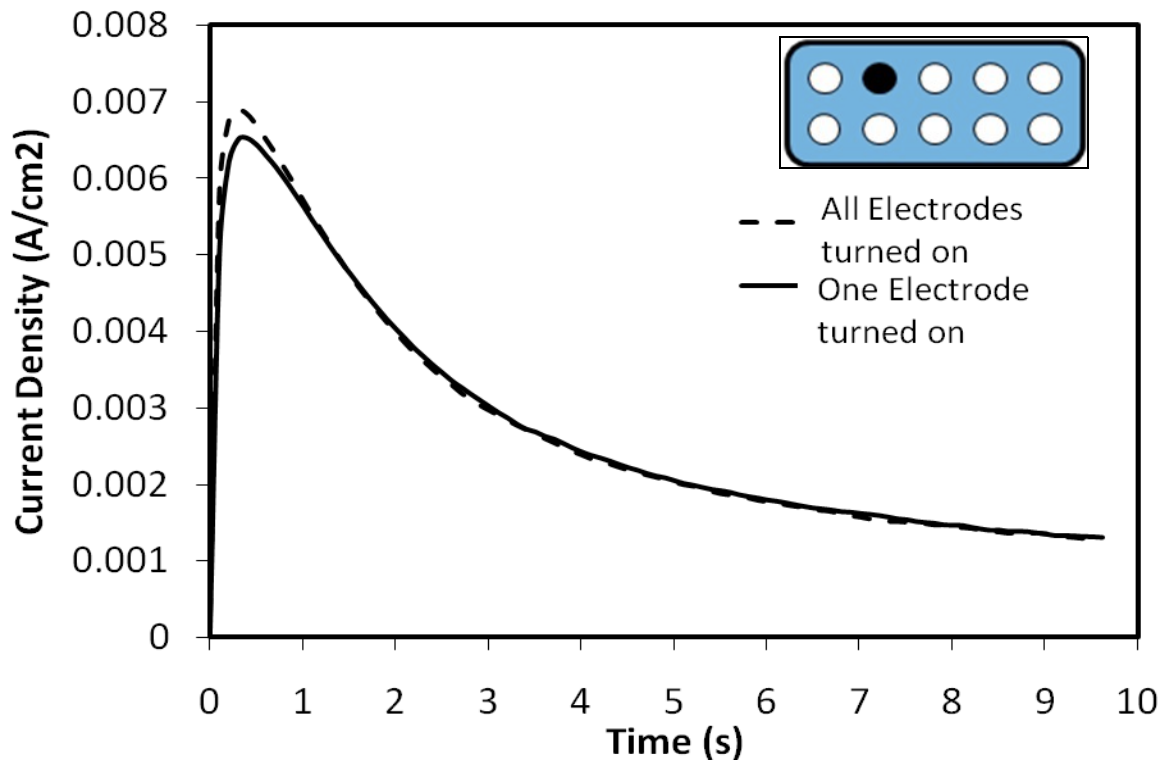


**Figure 3.** Current Response for a Single Electrode at 240 mV

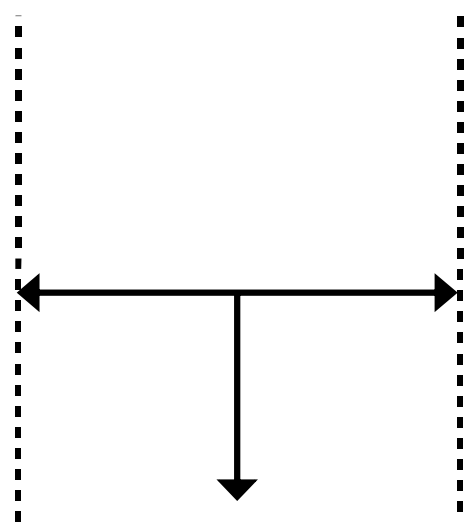
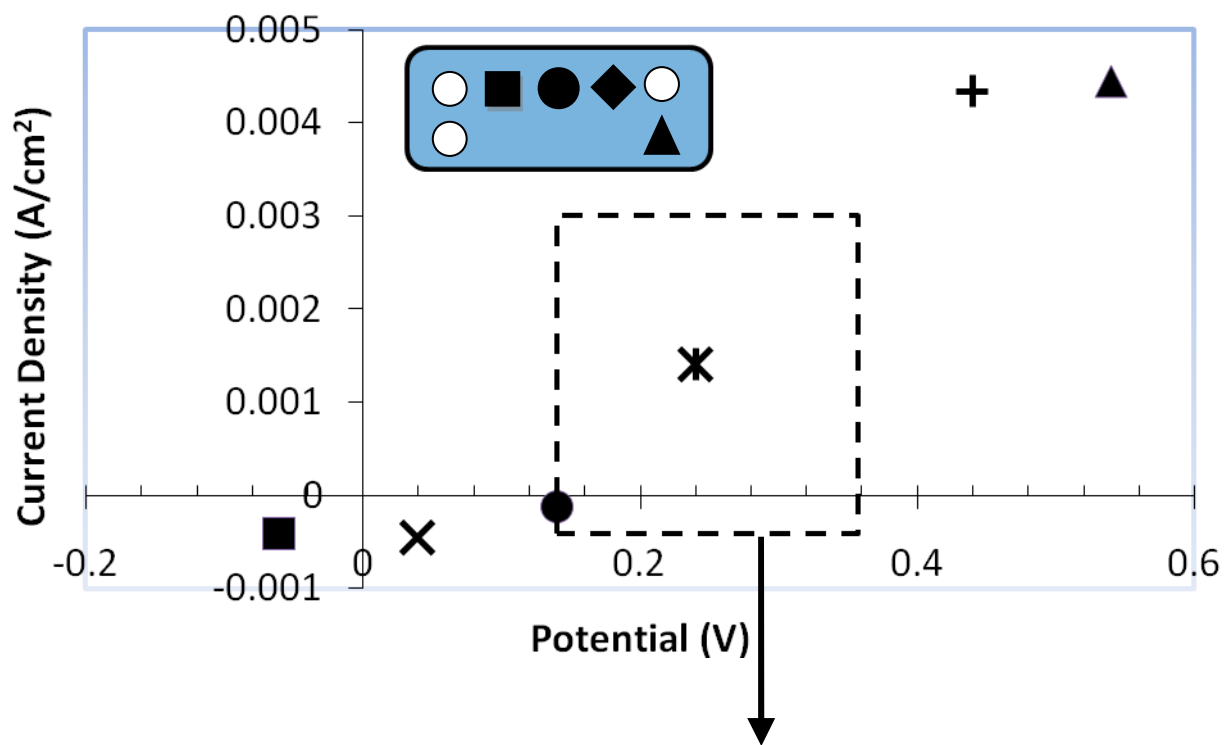
### *Sampled-Current Voltammetry:*

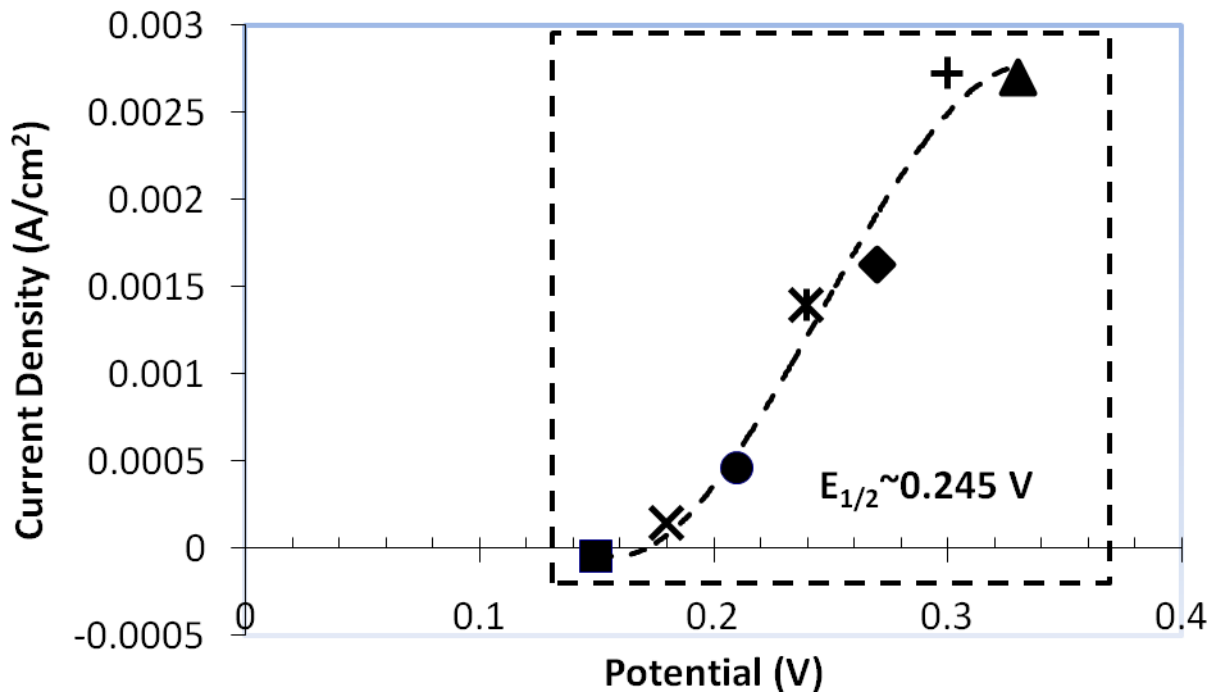
Next, the electrodes were activated simultaneously at different voltages with the current response measured by the MMA. The current data, sampled at 10 seconds for all electrodes, is plotted in Figure 4. The beginnings of an algorithm protocol for finding the  $E^{0'}$  can be seen here. First, multiple electrodes are used to sample the current over a large range of voltages that may include  $E^{0'}$ 's for several possible analytes. Then, by noting a large change in output current for a certain voltage span, the currents can be sampled again for a smaller potential window as seen in the second part of Figure 4. Once a small enough voltage range is reached, the half wave potential can be estimated. This was accomplished with a best fit model applied to the data and the middle voltage point found between the two peaks of the fit. The half-wave potential estimate is equivalent to the formal potential, because the diffusion coefficients are comparable for both forms of the redox couple ferro/ferricyanide.<sup>6</sup>

Sampling the current after waiting for a longer time resulted in a half-wave potential that was a closer estimate of the formal potential (Figure 5). The half-wave potential was found using the method introduced in Figure 4 and was based on data from multiple electrodes taken at different samples of time. Clearly, waiting for a longer time resulted in a better estimate of the formal potential. For example, at 60 seconds, the  $E^{0'}$  estimate is 0.237 V, which is in the range of formal potentials observed in cyclic voltammograms (0.22 V to 0.24 V).

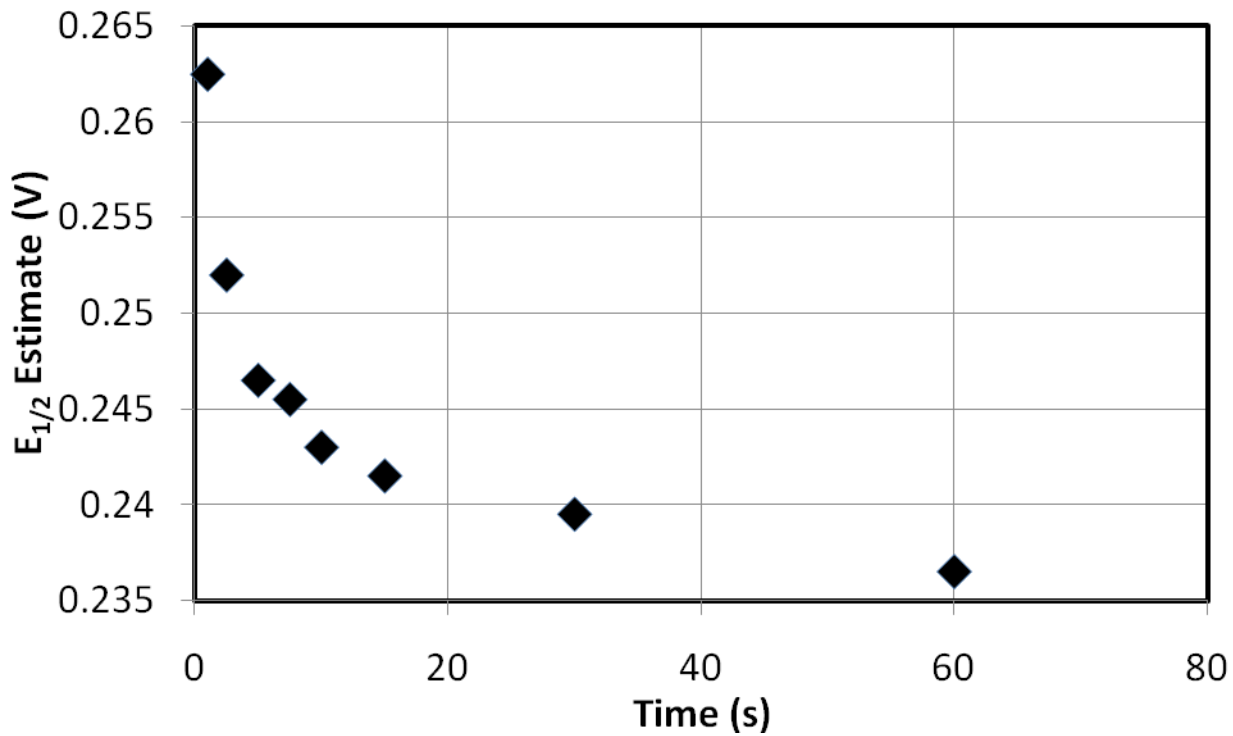
Another criterion to consider in the functionality of a sensor system is the minimum range of potentials sampled by the MMA with all of the electrodes. Figure 6 illustrates that as this minimum  $\Delta E$  between two electrodes increases, the estimation of the half wave potential deviates from  $E^{0'} \sim 0.22\text{-}0.24$  V. In other words, the closer the spacing between the potentials applied to different electrodes, the higher the precision for estimating the formal potential.

Figure 6 also reveals that waiting a longer time period, 10 seconds instead of 5, again results in a better estimate of  $E^0$ .





**Figure 4.** Sampled Current Voltammetric Measurements for Multiple Electrodes at Once Illustrating the Mechanism for Determining the  $E_{1/2}$



**Figure 5.** Formal Potential Estimate Over Time for Sampled Current Voltammetry Data

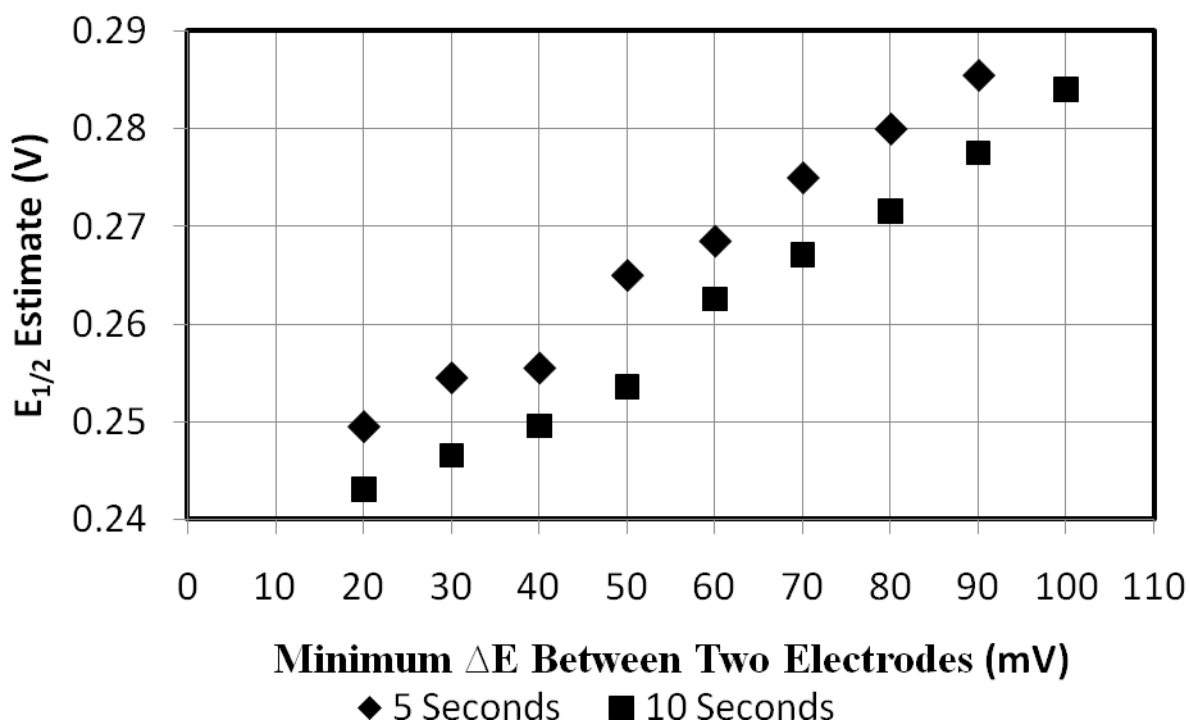


**Figure 6.** Formal Potential Estimate for Different Potential Intervals Between Electrodes

*Impedance Analysis:*

Next, the impedance magnitude was measured as a function of different polarization voltages and at frequencies of 5, 10, and 100 Hz (Figure 7). The impedance reaches a minimum at approximately 0.22 V for all the frequencies. This value corresponds to the expected formal potential which is again between 0.22 and 0.24 V according to CV scans. Also, the overall baseline for the impedance values seemed to decrease at higher frequencies.

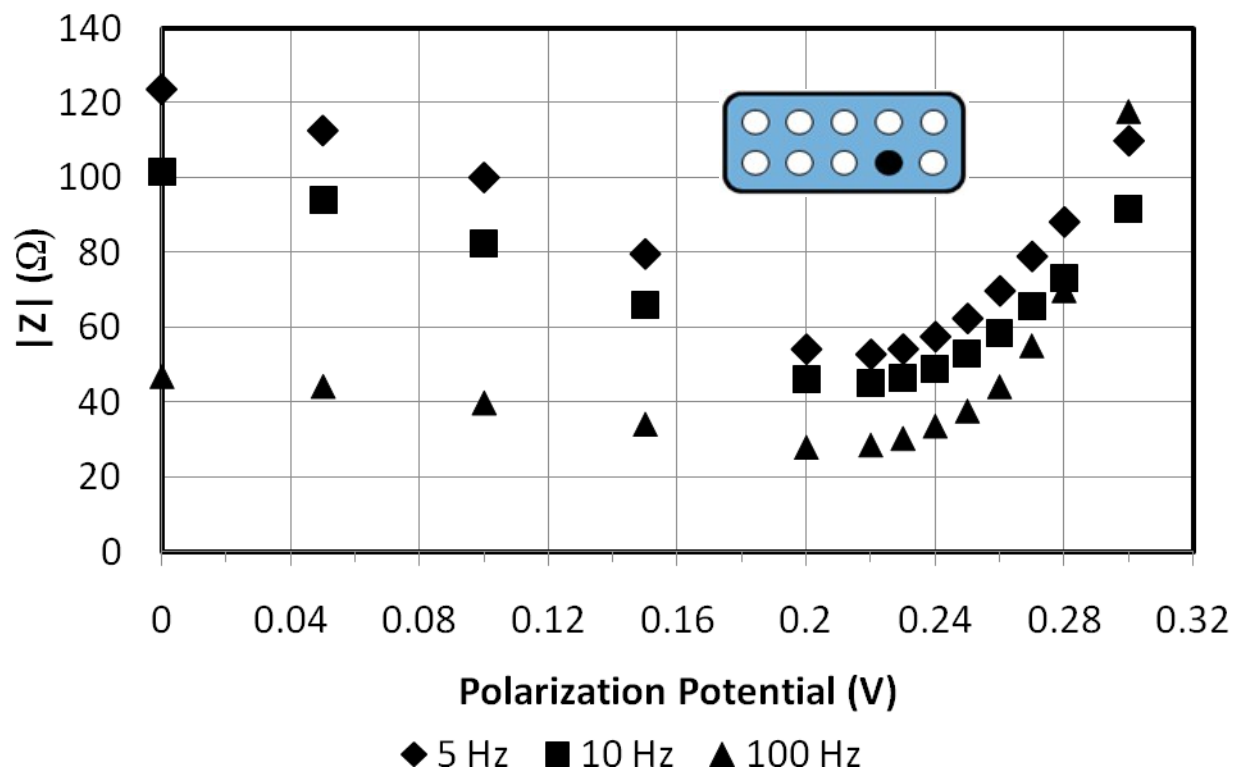


**Figure 7.** Impedance Measurements at Different Polarization Potentials and Frequencies

Lastly, concurrent application of polarization potentials was undertaken with the results shown in Figure 8. Just as was observed with the single electrode (Figure 7), monitoring multiple electrodes simultaneously also resulted in the impedance magnitude minimizing at 0.22 V or the  $E^{0'}$ . With this method, the determination of  $E^{0'}$  took approximately 10 seconds. Five seconds were required to establish the polarization potentials at the different electrodes and then it took 5 seconds to sweep the 15-17 Hz range. The impedance measurements in this frequency range seemed to reach a steady state with little noise.

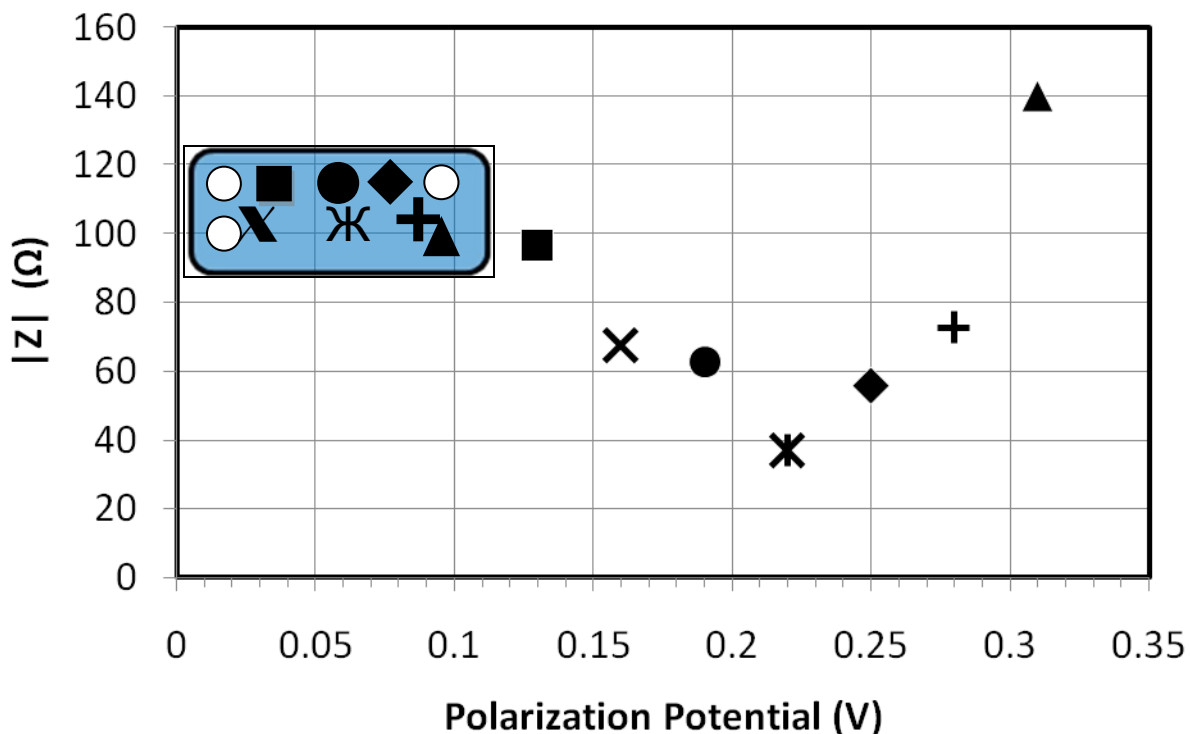


**Figure 8.** Impedance Measurements at Different Polarization Potentials and for an Impedance Sweep 15-17 Hz

#### 4. Discussion

##### *Crosstalk Check:*

Confirming that crosstalk is not a factor is vital in a sensor array system—especially in one where response is monitored at multiple electrodes that are millimeters apart. In the present electrode array, there appears to be minimal crosstalk between proximal electrodes. The diffusion layers around each electrode that are composed of either largely oxidized or reduced species do not seem to interfere with one another (Figure 3). The current-voltage (I-V) plots for a constant potential applied to all electrodes at once and to each electrode individually exhibited the same curvature characteristics. The small discrepancy in the initial rise in Figure 3 is likely attributed to a slight difference in the electrochemical cell conditions between trials and appears

to be a negligible result. In a sensing algorithm, the current values will never be acquired this early (<1 second) because some time has to be given for the solution to reach a level of steady state. Ultimately, the two fits that were applied showed an error of less than 1 percent between voltage application to individual electrodes and to all electrodes indicating that the diffusion regions of neighboring electrodes did not interfere with one another.

#### *Sampled-Current Voltammetry:*

The MMA could be programmed to establish recursive control of multiple electrodes to acquire current data in order to rapidly determine the  $E^{0'}$ . Figure 4 demonstrates the visualization of the way the MMA would be programmed. Numerous electrodes would be utilized to sample the current over a large range of voltages. Then, a zooming effect would be realized as a smaller range of potentials is tested in the area where a large change in current was seen in the previous scan. The half wave potential can eventually be estimated, and in turn, the formal potential. This technique could take on the order of tens of seconds to achieve that which a cyclic voltammogram takes several minutes to acquire.

Of course there are several factors to consider in order to conclusively find the  $E^{0'}$ . For instance, waiting a longer time and using smaller voltage intervals between electrodes allows for better estimate of the formal potential (Figures 5,6). Since the objective is to design a fast and responsive sensor, the sensing mechanism cannot wait sixty seconds to acquire potentiostatic current data at different electrodes. Thus, waiting for 5-10 seconds should be sufficient, as the  $E^{0'}$  estimate of  $\sim 0.245$  V here is a little above the actual formal potential of 0.24 V. The ideal  $\Delta E$  between electrodes to use seems to be 50 mV or less. The combination of waiting a long enough time and having small enough intervals between potentials applied to proximal electrodes approximates the formal potential closely to the actual value.

The ability to find the  $E^0$  in tens of seconds is especially applicable to a redox couple such as ferrocyanide. Reversible analytes are favorable as test elements because they usually yield products of the electrode reaction that are stable, and do not undergo further reactions in solution. Gold is likewise a favorable material for electrodes, because it experiences minimum adsorption interaction with the reactant ions in solution.<sup>10</sup> Also, the ferrocyanide exhibits approximately ideal quasi-reversible outer sphere kinetic behavior.<sup>14</sup> The electron transfer kinetics are rapid—resulting in a current that is directly proportional to the rate at which the analyte arrives at the electrode surface or is mass transport controlled.<sup>6</sup> The challenge in the development of future sensing systems will be to find electrochemical characteristics in analytes that are not ideal redox couples.

#### *Impedance Analysis:*

In addition to the sampled-current method, the present study attempted to determine the formal potential with impedance analysis. Figures 7 and 8 reveal that the minimum impedance is observed at a polarization potential approximately equal to the formal potential. The physical explanation for this phenomenon may be that the maximum change in output current occurs at the MMA input voltage equivalent the  $E^0$  polarization potential. After all, the MMA measures impedance as the input voltage change versus output current change  $\left(Z = \frac{\Delta V_{in}}{\Delta I_{out}}\right)$ . As evidenced by the cyclic voltammograms, the highest difference in output current occurs at a voltage equivalent to the formal potential. With a polarization potential equal to  $E^0$ , the AC voltage varies above and below it causing the measured current to drastically change—this results in a large  $\Delta I_{out}$ . Therefore, the lowest impedance should be observed at the formal potential where the change in measured input current is highest.

When multiple electrodes were employed simultaneously, it took 5 seconds to establish the different polarization potentials and 5 seconds to sweep from 17 to 15 Hz at each electrode. In a sensing algorithm, if the general location of an analyte's  $E^0$  is known, a voltage window of different offsets can be applied in order to look for the voltage location with the minimum impedance. The formal potential can thus be found in mere seconds. Moreover a similar algorithm can be used for impedometric measurements as was described for sampled-current voltammetry. First a large spectrum of polarization potentials can be applied to the system and then a smaller range based on where the impedance appears to be minimal.

## **5. Conclusion**

The study reveals that the Multichannel Microelectrode impedance Analyzer along with an electrode array can be a powerful combination in the goal of developing a fast sensor mechanism. Both the potentiometric and impedometric methods of operation led to determining the characterizing element of ferrocyanide, its formal potential, in approximately ten seconds. The traditional cyclic voltammetry technique takes several minutes to find the very same value. Granted, the sensing procedure was made easy by using a common redox element which has a very specific formal potential that defines the analyte. Still, these same techniques of applying different polarization potentials and measuring the current and impedance can be used on non-redox species to observe other electrochemical characteristics that differentiate those elements. Future work will focus on such non-ideal analytes. This study has been a crucial first step in developing a rapid electrochemical sensing system.

## **Acknowledgements**

We gratefully acknowledge contributions by Dr. Charles B. Parker and Dr. James B. Sund of Duke University and Dr. Brian Stoner at RTI International. This work was supported by the National Aeronautics and Space Administration (Dr. Seun Kahng, grant # NNL05AA14A) as well as the National Science Foundation (grant # ECS-0428540).

## References

- <sup>1</sup> Jawaheer S, Rughooputh HCS, White S, Cullen D. Development of an electrochemical sensor array for determination of food analytes, *Africon Conference in Africa, 2002. IEEE AFRICON. 6th*, vol.1, no., pp. 407-409 vol.1, 2-4 Oct. 2002
- <sup>2</sup> Krommenhoek EE, Gardeniers JG, Bomer JG, Li X, Ottens M, van Dedem GW, Van Leeuwen M, van Gulik WM, van der Wielen LA, Heijnen JJ, van den Berg AA. Integrated electrochemical sensor array for on-line monitoring of yeast fermentations. *Analytical chemistry* 2007;79(15):5567-73.
- <sup>3</sup> Chang SC, Pereira-Rodrigues N, Henderson JR, Cole A, Bedioui F, McNeil CJ. An electrochemical sensor array system for the direct, simultaneous in vitro monitoring of nitric oxide and superoxide production by cultured cells. *Biosensors & bioelectronics* 2005;21(6):917-22.
- <sup>4</sup> Bocher F. Coupled Multielectrode Investigation of Crevice Corrosion of AISI 316 Stainless Steel. *Electrochemical and solid-state letters* 2007;10(3):C16-.
- <sup>5</sup> Paeschke M. Voltammetric multichannel measurements using silicon fabricated microelectrode arrays. *Electroanalysis* 1996;8(10):891-.
- <sup>6</sup> Bard, AJ. Faulkner, LR. *Electrochemical Methods: Fundamentals and Applications*. Wiley. 2<sup>nd</sup> Edition. 2000.
- <sup>7</sup> Heras A. UV-Visible Spectroelectrochemical Detection of Side-Reactions in the Hexacyanoferrate (III)/(II) Electrode Process. *Electroanalysis* 2003;15(8):702-.
- <sup>8</sup> Zhang S, Wang N, Yu H, Niu Y, Sun C. Covalent attachment of glucose oxidase to an Au electrode modified with gold nanoparticles for use as glucose biosensor. *Bioelectrochemistry* 2005;67(1):15-22.
- <sup>9</sup> J. Youngsman, B. Marx, S. Wolter, J. Glass. and A.J. Moll, *Miniature Multi-electrode Electrochemical Cell in LTCC, IMAPS/ACerS Ceramic Interconnect and Ceramic Microsystems Technologies (CICMT)*, Denver, CO, April 25-27, 2006.
- <sup>10</sup> Lyons MEG. The Redox Behaviour of Randomly Dispersed Single Walled Carbon Nanotubes both in the Absence and in the Presence of Adsorbed Glucose Oxidase. *Sensors* 2006;6:1791-.
- <sup>11</sup> Zhang S, Wang N, Yu H, Niu Y, Sun C. Covalent attachment of glucose oxidase to an Au electrode modified with gold nanoparticles for use as glucose biosensor. *Bioelectrochemistry* 2005;67(1):15-22.
- <sup>12</sup> Janek RP. Impedance spectroscopy of self-assembled monolayers on Au (111): sodium ferrocyanide charge transfer at modified electrodes. *Langmuir* 1998;14(11):3011-.
- <sup>13</sup> Hill, B. Accu-Chek Advantage: Electrochemistry for Diabetes Management. *CurrentSeparations.com and Drug Development* 2005; 21(2).
- <sup>14</sup> Collyer SD. The electrochemistry of the ferri/ferrocyanide couple at a calix [4] resorcinarenetetra-thiol-modified gold electrode as a study of novel electrode modifying coatings for use within electro-analytical sensors. *Journal of electroanalytical chemistry and interfacial electrochemistry* 2003;549:119-.